

Article

# Redox Behavior and Electrochromism of a Viologen-Based Molten Poly(ionic liquid)

Hironobu Tahara<sup>1,2,\*</sup>, Saki Takuma<sup>2</sup>, Suguru Motokucho<sup>1,2</sup>, and Hiroto Murakami<sup>1,2,\*</sup>

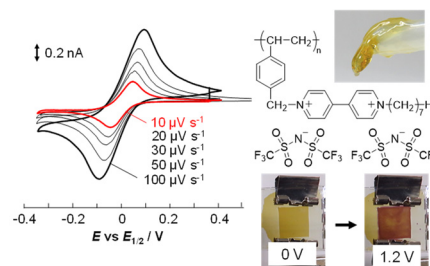
<sup>1</sup> Graduate School of Integrated Science and Technology, Nagasaki University 1-14 Bunkyo, Nagasaki 852-8521, Japan

<sup>2</sup> Graduate School of Engineering, Nagasaki University 1-14 Bunkyo, Nagasaki 852-8521, Japan

\* Correspondence: h-tahara@nagasaki-u.ac.jp (H.T.); hiroto@nagasaki-u.ac.jp (H.M.)

Received: 30 August 2025; Revised: 8 December 2025; Accepted: 14 December 2025; Published: 16 December 2025

**Abstract:** We present the synthesis and characterization of a viologen-based molten poly(ionic liquid), VPIL(TFSI), and its application to electrochromic (EC) devices. VPIL(TFSI) was obtained as a highly viscous liquid with a glass transition temperature of  $-23\text{ }^{\circ}\text{C}$ , enabling its use in a molten state without additional solvent. Electrochemical analysis by cyclic voltammetry (CV) and electrochemical impedance spectroscopy (EIS) of neat VPIL(TFSI) revealed a unique conduction mechanism: while ionic conductivity is dominated by the counter-anion (TFSI) migration, charge transport during redox cycling involves electron hopping between viologen units. Diffusion coefficient analysis indicated that electron hopping is slower than counter-anion migration, suggesting that the reorientation of viologen moieties, rather than ion migration, determines the transport kinetics. An EC device was fabricated using an equimolar mixture of VPIL(TFSI) and a ferrocene-based RAIL as cathodic and anodic components, respectively, without any supporting electrolyte. The device exhibited distinct coloration with strong absorption bands at 530 and 890 nm, attributed to  $\pi$ -dimerization of reduced viologen species, along with high contrast and coloration efficiency comparable to theoretical values. These findings demonstrate the potential of molten poly(ionic liquids) as promising redox-active media for solvent-free and durable electrochromic devices.



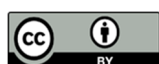
**Keywords:** redox-active ionic liquid; poly(ionic liquid); conducting polymer; electrochromism

## 1. Introduction

Ionic liquids (ILs) are often described as designer solvents [1] because their physicochemical properties, such as viscosity, ionic conductivity, melting point, and solubility, can be widely tuned. Redox-active ionic liquids (RAILs), a functional subclass of ILs, have attracted considerable attention as a new class of materials for electrochemical devices [2,3], since they can simultaneously serve as redox-active species, solvent, and supporting electrolyte. Compared with all-solid-state electrolytes, ILs generally offer higher ionic conductivity, better flexibility, and greater tunability. Consequently, RAILs have been applied to supercapacitors [4,5], redox flow batteries [6], and electrochromic (EC) devices [7,8], demonstrating new design concepts and good performance.

Organic-material-based EC devices have also been extensively developed owing to their flexibility, compatibility with solution processing, and tunable physicochemical and electronic properties through molecular design. Among them, diquatery salts of 4,4'-bipyridinium, commonly known as viologens, are well-established organic EC materials. Several viologen-based RAILs have been reported and investigated with respect to their electron transport properties and pronounced EC response [9–12]. EC devices employing viologen-based RAILs can operate without additional solvent and supporting electrolyte, thereby achieving improved durability by avoiding solvent evaporation, solution leakage, phase segregation, and component decomposition [8]. Nevertheless, demonstrations of such solvent- and electrolyte-free devices remain rare, because ionic redox-active species typically possess high melting points that are difficult to be lowered.

To expand the RAIL family, we have focused on poly(ionic liquid)s (PILs). PILs have received increasing attention due to their unique characteristics arising not only from their IL monomers but also from polymeric structural features rarely observed in conventional ILs [13–15]. Pioneering studies on the electrochemistry of redox-



**Copyright:** © 2025 by the authors. This is an open access article under the terms and conditions of the Creative Commons Attribution (CC BY) license (<https://creativecommons.org/licenses/by/4.0/>).

**Publisher's Note:** Scilight stays neutral with regard to jurisdictional claims in published maps and institutional affiliations.

active viologen-based PILs were reported by Ohno and co-workers [16], who elucidated their fundamental redox and conductive properties. Although several viologen-based polymers have been synthesized and studied [17–20], they have not been applied in the molten state. Thus, electrochromic devices incorporating viologen-based PILs without solvent or additional supporting electrolyte remain unexplored.

In this study, we describe the synthesis of a viologen-based PIL, investigate its charge transport properties, and demonstrate its application in a two-electrode EC device. The device employs a mixed RAIL system comprising a viologen-based PIL as the electrochromic cathodic component and a ferrocene-based RAIL as the anodic redox component, without solvent and supporting electrolyte. Even with VPIL(TFSI), high contrast and large absorbance were achieved, comparable to those of EC devices employing viologen-based ionic liquids reported in our previous work [7,8].

## 2. Materials

The ferrocene-based RAIL ([FcC<sub>6</sub>ImC<sub>1</sub>][TFSI], Figure 1a), used as a charge-compensating material for the reduction of VPIL, was synthesized according to a reported procedure [21]. The viologen-based PIL (VPIL(TFSI)) was prepared as outlined in Figure 1, with detailed procedures provided in the Supporting Information (SI). A viologen monomer bearing a styrene group at the terminal of the bipyridinium unit was first synthesized stepwise from 4,4'-bipyridyl. The viologen polymer, VPIL(X), was obtained by radical polymerization using potassium persulfate as the initiator. The water-soluble crude polymer was purified by dialysis (molecular weight cut-off  $1.4 \times 10^4$ ) to remove low-molecular-weight components. No residual monomer (StC<sub>1</sub>VC<sub>7</sub>) was detected in the purified product, as confirmed by <sup>1</sup>H NMR. Ion exchange of VPIL(X) to VPIL(TFSI) was achieved by treatment with LiTFSI in water. To eliminate residual halides, repeated liquid-liquid extraction with water and ethyl acetate was carried out until the aqueous layer no longer turned cloudy upon AgNO<sub>3</sub> testing. After evaporation of the ethyl acetate layer and careful drying under vacuum, a faint brown viscous liquid was obtained as VPIL(TFSI). The final product was characterized by <sup>1</sup>H NMR and energy-dispersive X-ray fluorescence spectroscopy to confirm the absence of residual monomer and halides, and the presence of the TFSI anion. The glass transition temperature was determined to be  $-23$  °C by differential scanning calorimetry (DSC) (Figure S1).

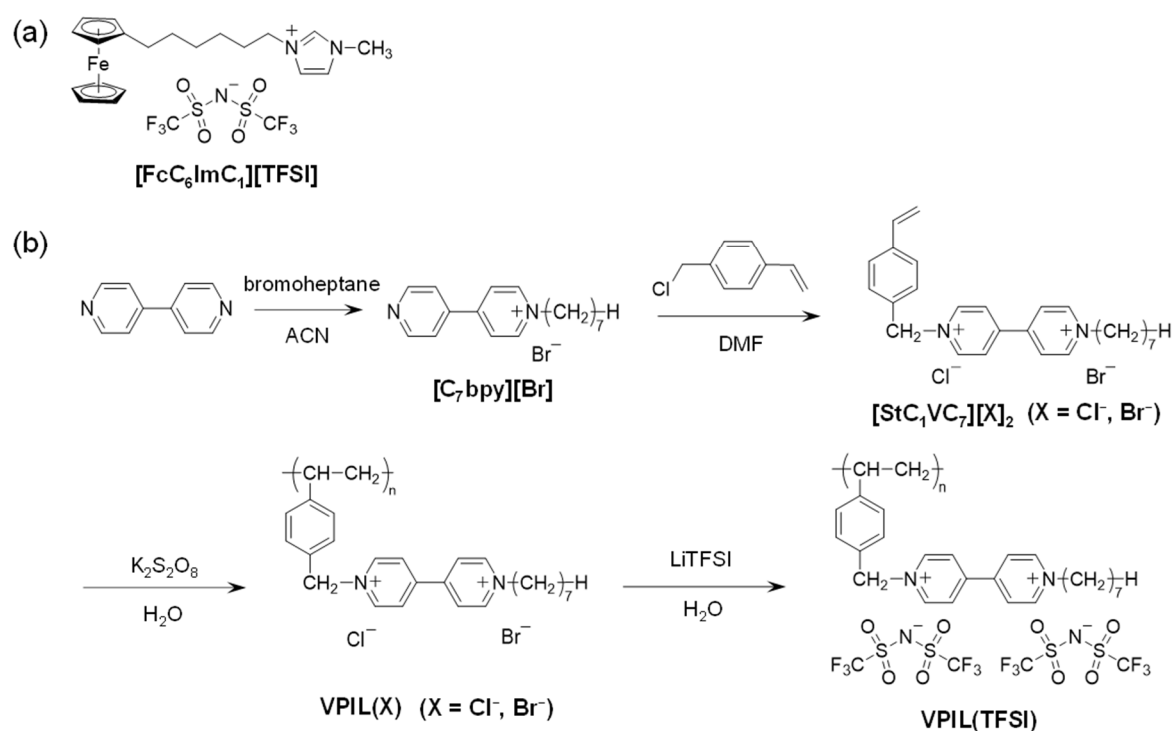


**Figure 1.** (a) Structure of [FcC<sub>6</sub>ImC<sub>1</sub>][TFSI]. (b) Synthetic scheme of VPIL(TFSI).

## 3. Measurement and Equipment

To evaluate the redox properties and charge transport characteristics of VPIL(TFSI), cyclic voltammetry and electrochemical impedance spectroscopy (EIS) were employed. The cell configuration for the cyclic voltammetry was the same as that reported in our previous study [22] (Figure 2a). A gold micro disk electrode with a diameter

of 100  $\mu\text{m}$  was used as a working electrode and platinum plate electrode was used as a counter electrode. The micro disk electrode experiment was carried out with a potentiostat (Huso (Kawasaki, Kanagawa, Japan), HECS 9094), a function generator (TEXIO Technology Corporation (Yokohama, Kanagawa, Japan), FGX-295), and a recorder (Yokogawa Test & Measurement Corporation (Hachioji, Tokyo, Japan), DL750). For the EIS measurements, a cell was constructed by sandwiching VPIL(TFSI) between two platinum plates, using a PTFE sheet (0.50 mm thick) with a 0.61  $\text{cm}^2$  hole as a separator. The sample was degassed under reduced pressure (15 Pa) at 90  $^\circ\text{C}$  to remove bubbles. For the evaluation of ionic conductivity, the cell constant was  $K_{\text{cell}} = 0.11 \text{ cm}^{-1}$ . EIS measurements were conducted using a lock-in amplifier (Edgerton, Germeshausen, and Grier, Inc. (Bedford, MA, USA), EG&G 7265) and a home-made potentiostat.

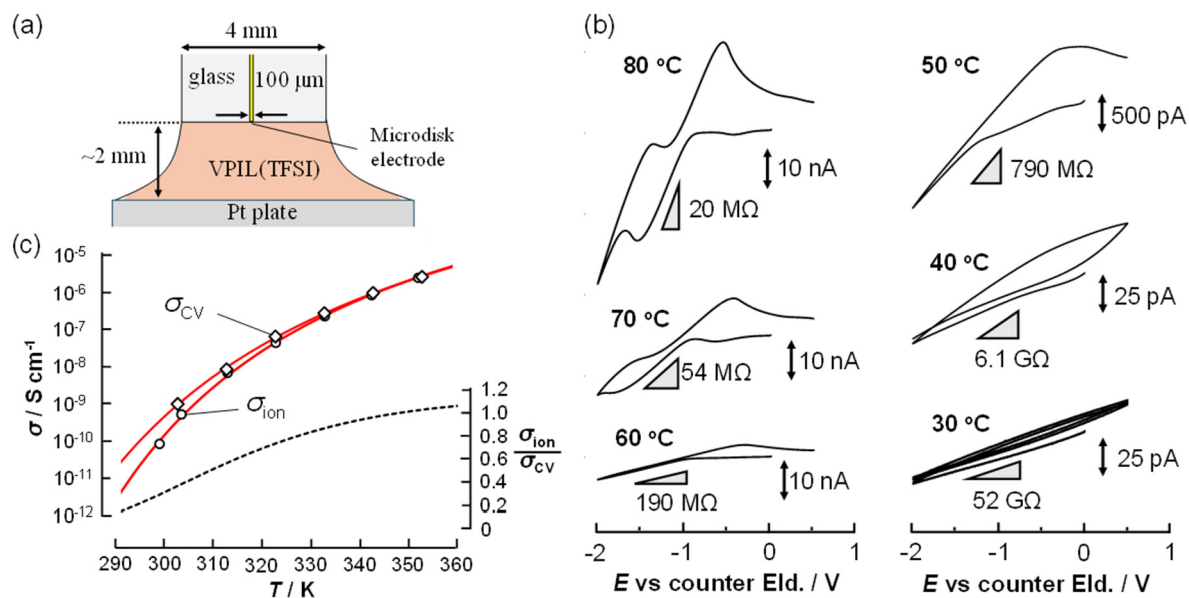


**Figure 2.** (a) Configuration of the CV experiment. The working electrode was Au microdisk electrode (diameter 100  $\mu\text{m}$ ) and the counter electrode was Pt plate. The overall setup was the same as our previous report [22]. (b) CVs ( $v = 100 \text{ mV}\cdot\text{s}^{-1}$ ) of VPIL(TFSI) at various temperatures (30–80  $^\circ\text{C}$ ). The triangles in the charts were the slope of the CVs in the straight-line region. The resistance values were the corresponding  $R_s$  values. (c) Conductivity of VPIL(TFSI) evaluated by AC impedance ( $\sigma_{\text{ion}}$ ,  $\circ$ ) and CV ( $\sigma_{\text{CV}}$ ,  $\diamond$ ) at various temperatures and the ratio of  $\sigma_{\text{ion}}$  and  $\sigma_{\text{CV}}$  (dashed line). Corresponding red lines were drawn using the VTF parameters in Table 1. The temperature dependence of  $\sigma_{\text{ion}}/\sigma_{\text{CV}}$  was plotted using the VFT parameters.

The EC device was fabricated following a procedure similar to that reported in our previous studies [7,8]. VPIL(TFSI) and  $[\text{FcC}_6\text{ImC}_1][\text{TFSI}]$  (Figure 1b) were mixed in a 1:1 molar ratio, calculated for VPIL(TFSI) on the basis of its viologen monomer units. A cleaned indium-tin-oxide (ITO) transparent electrode (GEOMATEC Co., Ltd. (Yokohama, Kanagawa, Japan), sheet resistance 10  $\Omega/\text{sq}$ , ITO thickness 200 nm) was laminated with a Himilan<sup>®</sup> ionomer film (25  $\mu\text{m}$  thick) containing a 1  $\text{cm} \times 1 \text{ cm}$  square aperture. The mixture of VPIL(TFSI) and  $[\text{FcC}_6\text{ImC}_1][\text{TFSI}]$  was then cast into the aperture, and the assembly was sealed by sandwiching with another bare ITO electrode to construct the EC device.

The EC experiment was carried out with a potentiostat (Huso (Kawasaki, Kanagawa, Japan), HECS 1110), a function generator (ToHo-TeCh (Yokohama, Kanagawa, Japan), FG-02), and a recorder (CONTEC (Osaka, Japan), AI-1664LAX-USB). Transmission absorption spectra were recorded by a multichannel spectrophotometer (Ocean Optics (Orlando, Florida, USA), HR4000CG-UV-NIR) with a Xe lamp (Ritu Oyo Kougaku Co., Ltd., (Niiza, Saitama, Japan)).

## 4. Results and Discussion

### 4.1. Conducting Properties of VPIL(TFSI)

Cyclic voltammograms (CVs) of VPIL(TFSI) were recorded at various temperatures using a two-electrode cell (Figure 2a). At 70  $^\circ\text{C}$  and 80  $^\circ\text{C}$ , the CVs obtained at 100  $\text{mV}\cdot\text{s}^{-1}$  exhibited peak-shaped waves (Figure 2b), characteristic of diffusion-controlled redox processes. At 60  $^\circ\text{C}$  and lower, however, the voltammograms became linear waveform, indicative of Ohmic behavior, in which the migration (drift) of redox-active ions is driven by the

potential gradient at the electrode surface. In this region, the current is dominated by migration and is independent of scan rate. The conductivity can be evaluated from the slope of the linear region according to Ohm's law:

$$R_s = \Delta E / \Delta I_{\text{mig}} \quad (1)$$

where  $R_s$  is the solution static resistance,  $\Delta I_{\text{mig}}$  is the change in migration current, and  $\Delta E$  is the electrode potential difference. The slopes of the CVs in the straight-line region directly correspond to the inverse number of  $\Delta E / \Delta I_{\text{mig}}$ . When the counter electrode is sufficiently large and placed far enough to surround the working electrode, the conductivity ( $\sigma_{\text{CV}}$ ) can be obtained from the electrode radius ( $r_e$ ) of the working electrode by the Newman equation [23]:

$$\sigma_{\text{CV}} = 1 / (4r_e R_s) \quad (2)$$

The  $\sigma_{\text{CV}}$  values were compared with the ionic conductivity ( $\sigma_{\text{ion}}$ ) obtained by AC impedance spectroscopy (Figure S2). Figure 2c shows the temperature dependence of  $\sigma_{\text{CV}}$ ,  $\sigma_{\text{ion}}$ , and  $\sigma_{\text{ion}}/\sigma_{\text{CV}}$  values. Both conductivities exhibited similar temperature dependence. Since  $\sigma_{\text{CV}}$  is measured during the redox process of viologen units at the electrode surface, it could reflect not only electron transfer at the electrode/VPIL(TFSI) interface but also electron hopping transport into the bulk coupled with counter-ion migration. Moreover, ionic conductivity is mainly attributed to TFSI migration ( $\sigma_{\text{ion}} \approx \sigma_{\text{TFSI}}$ ), because the viologen dication units are immobilized on the polymer backbone. In 60–80 °C range, the ratio  $\sigma_{\text{ion}}/\sigma_{\text{CV}}$  was approximately unity. Therefore, the electron hopping transport was limited solely by counter-ion migration at the temperature range. However, the observed ratio  $\sigma_{\text{ion}}/\sigma_{\text{CV}}$  was less than unity at lower temperatures and decreased further with decreasing temperature. This discrepancy likely reflects differences in phase constitution (formation of reduced phases) and transport mode (mixed-valence conduction), resulting in higher conductivity in the CV experiment than the ionic conductivity of TFSI species. That is, at low temperatures, the macroscopic motion of counter ions is significantly restricted, whereas electron hopping, which involves short-range electron transfer driven by microscopic reorientation, can remain effective. Furthermore, a reduced phase composed of oxidized and reduced viologen species, i.e., a mixed-valence phase, may be stabilized at lower temperatures. The pronounced difference observed for VPIL(TFSI) suggests a distinctive charge-transport mechanism arising from the immobilization of the redox-active viologen units on the polymer backbone.

The Arrhenius plots of conductivity were nonlinear (Figure S3) and could be fitted by the Vogel-Fulcher-Tammann (VFT) equation:

$$\sigma(T) = \sigma_0 \exp\left(\frac{B}{T - T_0}\right) \quad (3)$$

The fitted parameters are summarized in Table 1. The  $T_0$  values obtained from  $\sigma_{\text{ion}}$  and  $\sigma_{\text{CV}}$  were close to each other and slightly lower than the glass transition temperature of VPIL(TFSI) (−23 °C, 250 K), consistent with their origin from the same  $T_g$ . At lower temperatures, the enhanced contribution from mixed-valence conduction could be attributed to the prolonged lifetime of reduced states formed near the electrode surface under higher viscosity.

**Table 1.** VFT parameters of  $\sigma_{\text{CV}}$  and  $\sigma_{\text{ion}}$ .

	$\sigma_{\text{CV}}$	$\sigma_{\text{ion}}$
$\ln(\sigma_0/\text{S}\cdot\text{cm}^{-1})$	−0.3839	−1.080
$B/\text{K}$	1601	1453
$T_0/\text{K}$	224.6	211.5

The apparent diffusion coefficient ( $D_{\text{app}}$ ), which includes contributions from both physical diffusion and electron hopping diffusion, is a key electrochemical parameter for concentrated redox systems. Murray and co-workers reported extremely low diffusion coefficients for undiluted redox melts without solvent and supporting electrolyte, obtaining reversible CVs only at very slow scan rates ( $50 \mu\text{V}\cdot\text{s}^{-1}$ ) [24]. Similarly, we observed quasi-reversible CVs for VPIL(TFSI) when the scan rate was decreased stepwise (Figure 3a,b). The peak-to-peak separation ( $\Delta E_p$ ) decreased with decreasing scan rate, reaching 91 mV at  $10 \mu\text{V}\cdot\text{s}^{-1}$  at 70 °C (Figure 3c). The linear dependence of peak current ( $i_p$ ) on the square root of scan rate ( $v^{1/2}$ ) indicated planar diffusion behavior. Incidentally, the measurement time was too long to collect the temperature dependence data. The diffusion coefficient was evaluated from the Randles–Ševčík equation:

$$i_p = 0.4463 nFAc \sqrt{\frac{nFDv}{RT}} \quad (4)$$

where  $n$ ,  $F$ ,  $A$ ,  $c$ ,  $D$ ,  $v$ ,  $R$ , and  $T$  are the number of electrons, the Faraday constant, electrode area, concentration of redox species in the bulk, diffusion coefficient, scan rate, gas constant, and absolute temperature, respectively. In general, Equation (4) is applicable under purely diffusional conditions, i.e., in supporting electrolyte-containing solutions where migration currents are suppressed. In the case of the VPIL(TFSI) system, although no supporting electrolyte was added, Equation (4) was applied to estimate  $D_{app}$  value, because  $i_p$  and  $v^{1/2}$  exhibited a good linear relationship at lower scan rates. As the result,  $D_{app}$  was calculated to be  $2.2 \times 10^{-11} \text{ cm}^2 \cdot \text{s}^{-1}$  ( $2.4 \times 10^{-11} \text{ cm}^2 \cdot \text{s}^{-1}$  for the anodic process and  $2.0 \times 10^{-11} \text{ cm}^2 \cdot \text{s}^{-1}$  for the cathodic process), assuming a redox-site concentration of  $c_V = 1.0 \text{ mol} \cdot \text{L}^{-1}$  at  $70^\circ \text{C}$ .

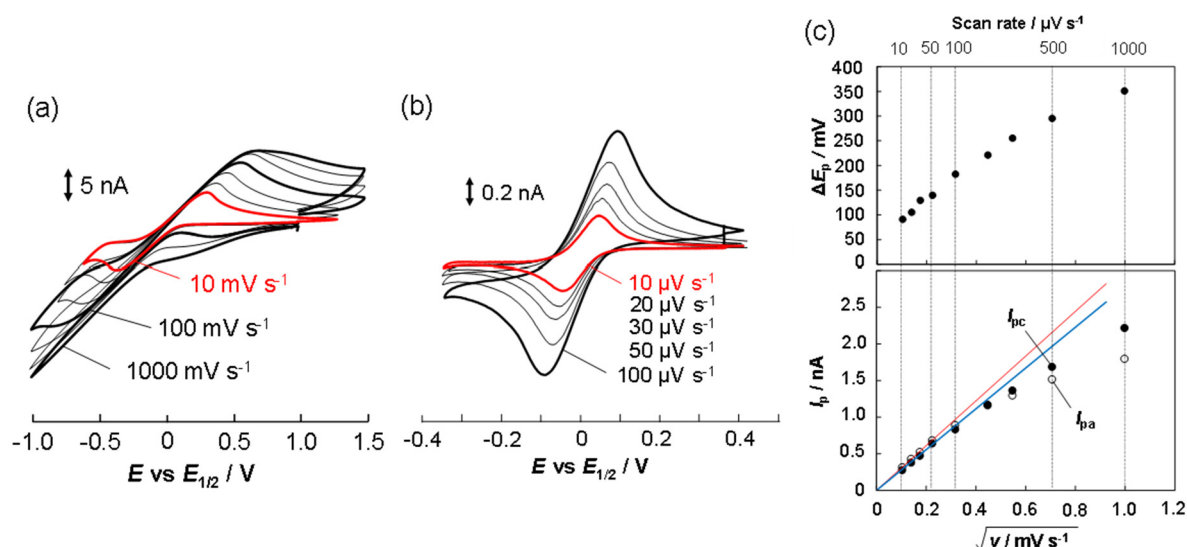
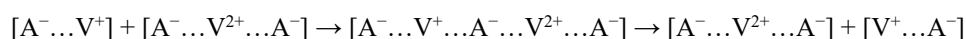


**Figure 3.** CVs and peak current analysis of VPIL(TFSI) at  $70^\circ \text{C}$  with various scan rates. (a) CVs at the higher scan rates region. (b) CVs at the slower scan rate region. (c) Scan rate dependence of the peak separation ( $\Delta E$ ) and the peak currents ( $I_p$ ) at  $70^\circ \text{C}$ . The red and blue lines are the slopes in cathodic and anodic peak currents, respectively.

According to the Dahms-Ruff model [25–27],  $D_{app}$  is the sum of physical diffusion coefficient ( $D_{phys}$ ) and electron hopping diffusion coefficient ( $D_{hop}$ ). Because the viologen redox sites are covalently bound to the polymer backbone,  $D_{phys}$  is negligible, and  $D_{app} \approx D_{hop}$ . However, since migration effects (the enhancement of electron hopping by potential gradients) were not considered, the obtained  $D_{hop}$  is expected to be overestimated. The extent of this overestimation can be estimated from the ionic conductivity of the counter ion, as expressed by the Nernst-Einstein relation:

$$\sigma = \frac{F^2}{RT} \sum_i z_i^2 c_i D_i \quad (4)$$

where  $z_i$ ,  $c_i$ , and  $D_i$  are the charge, concentration, and diffusion coefficient of species  $i$ , respectively. As previously mentioned, ionic conductivity is effectively governed by TFSI transport ( $\sigma_{ion} \approx \sigma_{TFSI}$ ). At  $70^\circ \text{C}$ ,  $D_{TFSI}$  was  $7.7 \times 10^{-11} \text{ cm}^2 \cdot \text{s}^{-1}$  with  $c_{TFSI} = 2.0 \text{ M}$ . Since  $D_{TFSI}$  was 3.5 times larger than the measured  $D_{hop}$ , even when migration contributions were included,  $D_{hop}$  is presumed to be overestimated by several tens of percent. It is very difficult to quantitatively estimate migration contribution. However, according to steady-state theory of Hyk and Stojek [22,28],  $D_{hop}$  is overestimated by approximately 27% in the absence of supporting electrolyte and one-electron reduction of a dicationic redox species. This theory can also be applied to quasi-steady-state conditions, such as cyclic voltammetry at slow scan rates [22]. In addition, as reported by Savéant and co-workers, this estimation is considered to be valid [29]. Therefore, since  $D_{TFSI}$  is approximately five times greater than true  $D_{hop}$ , the apparent value of  $D_{hop}$  obtained experimentally is overestimated due to the migration effect. The electron-hopping scheme between reduced viologen ( $V^+$ ) and oxidized viologen ( $V^{2+}$ ), accompanied by counter anion  $A^-$  movement under charge-neutrality condition described as follows:



When counter anion movement is sufficiently fast, it efficiently neutralizes the charge of the viologen species, allowing electron hopping to proceed smoothly. Thus, the rate-determining step for electron hopping reaction in VPIL(TFSI) is more likely the reorientation of viologen units, rather than counter-ion migration.

## 4.2. Application to EC Device

VPIL(TFSI) was employed as the active material in an EC device. The single liquid layer consisted of an equimolar mixture of VPIL(TFSI) (calculated on a viologen unit basis) and  $[\text{FcC}_6\text{ImC}_1][\text{TFSI}]$ . CV of the EC device is shown in Figure 4a. A driving voltage of 1.2 V was selected, which corresponds to the potential range of the one-electron oxidation of ferrocene and the one-electron reduction of viologen [7,8]. Figure 4b presents the difference absorbance spectra, defined as  $\Delta\text{Abs}(1.2\text{ V}) = -\log(I(1.2\text{ V})/I(0\text{ V}))$ , where  $I(E)$  is the transmitted light intensity at voltage  $E$ . Two characteristic absorption bands appeared at 530 and 890 nm, indicative of the formation of  $\pi$ -dimerized reduced viologen units. In contrast to our previous reports [7,8], no band was observed at 600 nm, confirming the absence of monomeric viologen radical species. Initially, the EC device appeared light yellow due to the ferrocene, but upon applying 1.2 V it turned reddish purple, originating from the reduced viologen (Figure 4c).

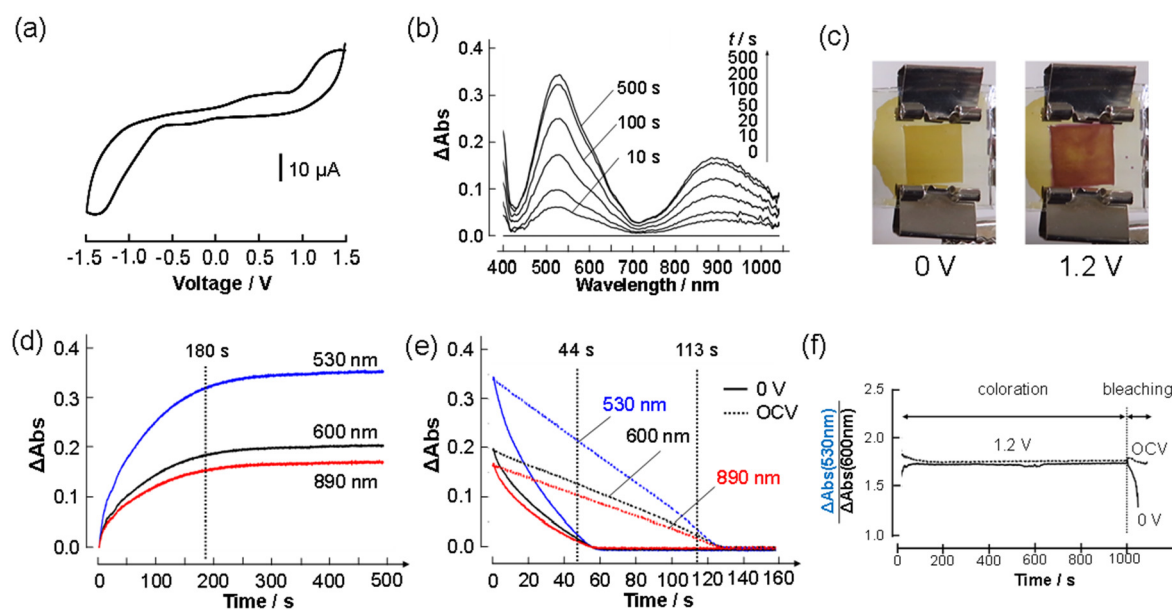


**Figure 4.** Electrochemical and spectro-electrochemical response of the EC device using VPIL(TFSI) and  $[\text{FcC}_6\text{ImC}_1][\text{TFSI}]$  at 298 K. (a) Cyclic voltammogram at  $20\text{ mV}\cdot\text{s}^{-1}$ . (b) Absorption spectrum changes under electrolysis at 1.2 V. (c) Photo images of the EC device at 0 V and 1.2 V. (d,e) Time course of absorbance changes at characteristic wavelengths in coloring process at 1.2 V and bleaching process at 0 V and OCV. (f) Time course of the absorbance ratio at 530 nm and 600 nm in coloring (0 V to 1.2 V) and bleaching (1.2 V to 0 V and OCV) process.

Figure 4d,e show the time-dependent optical response during potential steps from 0 to 1.2 V (coloration) and back to 0 V and open circuit condition (bleaching). The coloration reached a steady state around 180 s (time to reach 90% absorbance change of steady state) at 1.2 V and proceeded under diffusion-controlled kinetics, as evidenced by the proportionality of absorbance to the square root of time (Figure S4a). Because of the greater IR drop in this system, a higher driving voltage (1.2 V) was required compared with our previous study (1.0 V) [7,8]. Bleaching required 44 s at 0 V and 113 s under open-circuit conditions, defined as the time needed to recover 90% of the initial state (see the supporting information video). In contrast, in our previous EC device based on a mixture of viologen-based and ferrocene-based RAILs [8], coloration reached a steady state within 26 s at 1.0 V, and bleaching required 12 s at 0 V and 45 s under open-circuit conditions. These can be attributed to the extremely high viscosity of the VPIL(TFSI)/ $[\text{FcC}_6\text{ImC}_1][\text{TFSI}]$  mixture, retarding the transport of redox species. This slow bleaching rate contributes to the memory effect of coloration, namely the persistence of the colored state even in the absence of an applied voltage. Increasing the viscosity of the solution and controlling the deposition behavior of the EC species on the electrode surface are considered effective strategies for enhancing the memory effect. However, careful design is required, as excessive deposition can also diminish the reversibility of the EC device. The absorbance ratio  $\Delta\text{Abs}(530\text{ nm})/\Delta\text{Abs}(600\text{ nm})$  remained constant during both coloring and bleaching (Figure 4f), suggesting that  $\pi$ -dimerization occurs much faster than the electrode reaction. This can be rationalized by the fact that the viologen units in VPIL(TFSI) are fixed to the polymer backbone, enabling reduced viologens to aggregate rapidly and efficiently. However, this aggregation behavior does not always have a positive effect on the EC device. The coloration and bleaching response during voltage cycling between 0 and 1.2 V gradually deteriorated, and noticeable color non-uniformity appeared after approximately 700 cycles (Figure S6). This degradation is

likely associated with the aggregation behavior of VPIL. The observed color non-uniformity suggests that the reduced viologen species are distributed unevenly in the solution, resulting in non-uniform conductivity. In fact, such non-uniform coloration was not observed in the system using a mixture of viologen-based RAIL and [FcC<sub>6</sub>ImC<sub>1</sub>][TFSI]. PILs can form various structures, which can be tuned by solvents or coexisting components [13–15]. In this study, we did not focus on optimizing the solvent or coexisting materials for VPIL(TFSI) to control its solubility and structural organization in the solution. Therefore, it will be necessary to develop a suitable coexisting component (e.g., a counter-electrode reactant or a solvent—only [FcC<sub>6</sub>ImC<sub>1</sub>][TFSI] was used in this study) that can dissolve the reduced form of VPIL(TFSI) uniformly in order to maintain high conductivity in the PIL-based system.

The coloration efficiency, defined as  $\eta(\lambda) = \Delta\text{Abs}(\lambda)/Q$ , was evaluated to be 118 cm<sup>2</sup>·C<sup>-1</sup> from the slope of the charge- $\Delta\text{Abs}$  relationship at the initial stage of redox process (Figure S4c). The maximum coloration efficiency of the EC device can be described with molar absorption coefficient of the EC species according to the following equation [30]:

$$\eta_{\text{max}} = 1000 \frac{\Delta\varepsilon(\lambda)}{F} \quad (5)$$

where  $\Delta\varepsilon(\lambda)$  is molar absorption coefficient changes of electrochromic species both on anode and cathode and  $F$  is Faraday constant. The typical molar absorption coefficients of ferrocene are 100 M<sup>-1</sup>·cm<sup>-1</sup> at 440 nm in reduced form (Fc<sup>0</sup>) and 425 M<sup>-1</sup>·cm<sup>-1</sup> around 620 nm in oxidized form (Fc<sup>+</sup>) [31], and those of viologen are zero around visible region in oxidized form (V<sup>2+</sup>), 1.0–1.4 × 10<sup>4</sup> M<sup>-1</sup>·cm<sup>-1</sup> around 600 nm in reduced monomer form (V<sup>+</sup>), and 0.85–3.2 × 10<sup>4</sup> M<sup>-1</sup>·cm<sup>-1</sup> around 550 nm in the reduced  $\pi$ -dimer form (V<sup>+</sup>) [32]. Those values give a practical approximation of  $\Delta\varepsilon(\lambda) = (\varepsilon_{V^+}(\lambda) - \varepsilon_{V^{2+}}(\lambda)) - (\varepsilon_{Fc^+}(\lambda) - \varepsilon_{Fc^0}(\lambda)) \approx \varepsilon_{V^+}(\lambda)$ , resulting in  $\eta_{\text{max}} = 140$  cm<sup>2</sup>·C<sup>-1</sup> around 600 nm in the monomer form and 160 cm<sup>2</sup>·C<sup>-1</sup> around 550 nm in the  $\pi$ -dimer form. The experimental coloration efficiencies were 118 cm<sup>2</sup>·C<sup>-1</sup> at 530 nm, 73 cm<sup>2</sup>·C<sup>-1</sup> at 600 nm, and 55 cm<sup>2</sup>·C<sup>-1</sup> at 890 nm comparable to the theoretical value. By comparison with the EC devices based on viologen polymers and ferrocenes [33,34], coloration efficiency in this study was comparable. Thus, by utilizing VPIL(TFSI), we successfully fabricated an EC device exhibiting sharp contrast and high coloration efficiency. Again, EC device using VPIL(TFSI)

## 5. Conclusions

In this study, we demonstrated that a viologen-based molten poly(ionic liquid), VPIL(TFSI), can serve as a redox-active medium with distinctive charge transport properties and practical applicability in an EC device. Electrochemical analyses revealed that the conductivity of VPIL(TFSI) originates from electron hopping coupled with counter-ion migration, while diffusion coefficient evaluation suggested that the rate-determining step is the reorientation of viologen sites rather than ion transport. The combination of VPIL(TFSI) with a ferrocene-based RAIL enabled the fabrication of an EC device that operates without solvent and supporting electrolyte. The device exhibited reversible coloration with strong absorption associated with  $\pi$ -dimerized viologen species and delivered coloration efficiencies comparable to theoretical expectations. The use of VPIL(TFSI) in EC devices offers significant advantages. While the electronic conductivity of VPIL(TFSI) contributes positively to device performance, the tendency of viologen units to aggregate can adversely affect color uniformity. Therefore, the development of suitable cosolvents or counter-electrode coexistence materials that suppress aggregation is highly desirable. These findings highlight the potential of molten poly(ionic liquids) as a new platform for solvent-free, durable, and efficient redox-active systems, offering a promising design strategy for next-generation electrochromic and related electrochemical devices.

**Supplementary Materials:** The following supporting information can be downloaded at: <https://media.sciltp.com/articles/others/2512161608182500/MI-25080353-SI.zip>. Materials and Synthesis of VPIL(TFSI); Figure S1: DSC thermogram of VPIL(TFSI); Figure S2: EIS experiment; Figure S3: Arrhenius plot of  $\sigma_{cv}$  and  $\sigma_{imp}$ ; Figure S4: Coloration kinetics and coloration efficiency of the EC device; Figure S5: Potential step durability test; Figure S6: Photo image of the EC device after 700th voltage cycling. Video S1: Coloration of EC device by the voltage of 1.2 V.

**Author Contributions:** H.T.: conceptualization, methodology, data curation, funding acquisition, writing—original draft preparation, investigation; S.T.: synthesis; S.M.: methodology; H.M.: investigation, data curation, funding acquisition, writing—reviewing and editing. All authors have read and agreed to the published version of the manuscript.

**Funding:** This work was supported by a Japan Society for the Promotion of Science (JSPS) Grant-in-Aid for Young Scientists (B) No. 26810052 (H.T.), Grant-in-Aid for Scientific Research (C) No. 20K05649 (H.T.), and 22K05258 (H.M.).

**Data Availability Statement:** Not applicable.

**Acknowledgments:** This work was the result of using research equipment (<sup>1</sup>H NMR, elemental analysis, mass spectroscopy) shared in MEXT Project for promoting public utilization of advanced research infrastructure (Program for supporting introduction of the new sharing system) Grant Number JPMXS0422500320.

**Conflicts of Interest:** The authors declare no conflict of interest.

**Use of AI and AI-Assisted Technologies:** No AI tools were utilized for this paper.

## References

1. Freemantle, M. Designer Solvents. *Chem. Eng. News* **1998**, *76*, 32–37.
2. Doherty, A.P. Redox-active ionic liquids for energy harvesting and storage applications. *Curr. Opin. Electrochem.* **2018**, *7*, 61–65.
3. Rochefort, D. Enabling new electrochemical methods with redox-active ionic liquids. *Curr. Opin. Electrochem.* **2019**, *15*, 125–132.
4. Xie, H.J.; Gelinas, B.; Rochefort, D. Redox-active electrolyte supercapacitors using electroactive ionic liquids. *Electrochim. Commun.* **2016**, *66*, 42–45.
5. Mourad, E.; Coustan, L.; Lannelongue, P.; Zigah, D.; Medhdi, A.; Vioux, A.; Freunberger, S.A.; Favier, F.; Fontaine, O. Biredox ionic liquids with solid-like redox density in the liquid state for high-energy supercapacitors. *Nature Mater.* **2017**, *16*, 446.
6. Takechi, K.; Kato, Y.; Hase, Y. A Highly Concentrated Catholyte Based on a Solvate Ionic Liquid for Rechargeable Flow Batteries. *Adv. Mater.* **2015**, *27*, 2501–2506.
7. Tahara, H.; Baba, R.; Iwanaga, K.; Sagara, T.; Murakami, H. Electrochromism of a bipolar reversible redox-active ferrocene–viologen linked ionic liquid. *Chem. Commun.* **2017**, *53*, 2455–2458.
8. Tahara, H.; Uranaka, K.; Hirano, M.; Ikeda, T.; Sagara, T.; Murakami, H. Electrochromism of Ferrocene- and Viologen-Based Redox-Active Ionic Liquids Composite. *ACS Appl. Mater. Interfaces* **2019**, *11*, 1–6.
9. Hatazawa, T.; Terrill, R.H.; Murray, R.W. Microelectrode Voltammetry and Electron Transport in an Undiluted Room Temperature Melt of an Oligo(ethylene glycol)-Tailed Viologen. *Anal. Chem.* **1996**, *68*, 507–603.
10. Causin, V.; Saielli, G. Effect of asymmetric substitution on the mesomorphic behaviour of low-melting viologen salts of bis(trifluoromethanesulfonyl)amide. *J. Mater. Chem.* **2009**, *19*, 9153–9162.
11. Jordao, N.; Cabrita, L.; Pina, F.; Branco, L. Novel Bipyridinium Ionic Liquids as Liquid Electrochromic Devices. *Chem. Eur. J.* **2014**, *20*, 3982–3988.
12. Bodappa, N.; Broekmann, P.; Fu, Y.-C.; Furrer, J.; Furue, Y.; Sagara, T.; Siegenthaler, H.; Tahara, H.; Veszteg, S.; Zick, K.; et al. Temperature-Dependent Transport Properties of a Redox-Active Ionic Liquid with a Viologen Group. *J. Phys. Chem. C* **2015**, *119*, 1067–1077.
13. Yuan, J.; Mecerreyes, D.; Antonietti, M. Poly(ionic liquids): An update. *Progress in Polym. Sci.* **2013**, *38*, 1009–1036.
14. Qian, W.; Texter, J.; Yan, F. Frontiers in poly(ionic liquids): Syntheses and applications *Chem. Soc. Rev.* **2017**, *46*, 1124–1159.
15. Zhang, S.-Y.; Zhuang, Q.; Zhang, M.; Wang, H.; Gao, Z.; Yuan, J. Poly(ionic liquid) composites. *Chem. Soc. Rev.* **2020**, *49*, 1726–1755.
16. Ito, K.; Ohno, H. Polyether/salt hybrid: 5. Phase and bulk electrochemical response of viologens having poly(ethylene oxide) chain. *Polymer* **1997**, *38*, 921–926.
17. Chen, F.; Ren, Y.; Guo, J.; Yan, F. Thermo- and Electro-Dual Responsive Poly(ionic liquid) Electrolyte Based Smart Windows. *Chem. Commun.* **2017**, *53*, 1595–1598.
18. Burgess, M.; Chénard, E.; Hernández-Burgos, K.; Nagarjuna, G.; Assary, R.S.; Hui, J.; Moore, J.S.; Rodríguez-López, J. Impact of Backbone Tether Length and Structure on the Electrochemical Performance of Viologen Redox Active Polymers. *Chem. Mater.* **2016**, *28*, 7362–7374.
19. Greene, A.F.; Danielson, M.K.; Delawder, A.O.; Liles, K.P.; Li, X.; Natraj, A.; Wellen, A.; Barnes, J.C. Redox-Responsive Artificial Molecular Muscles: Reversible Radical-Based Self-Assembly for Actuating Hydrogels. *Chem. Mater.* **2017**, *29*, 9498–9508.
20. In, Y.; Park, H.; Kwon, J.; Kim, Y.; Kim, K.-W.; Pathak, D.; Kim, S.; Lee, S.; Moon, H. Isomeric effects of polyviologens on electrochromic performance and applications in low-power electrochemical devices. *Sol. Energy Mater. Sol. Cells* **2022**, *240*, 111734.
21. Gharib, B.; Hirsch, A. Synthesis and Characterization of New Ferrocene-Containing Ionic Liquids. *J. Org. Chem.* **2014**, *2014*, 4123–4136.
22. Tahara, H.; Miyaji, M.; Murakami, H.; Sagara, T. Determination Method of Diffusion Coefficient in a Neat Redox-Active Ionic Liquid at a Microdisk Electrode in the Domains Ranging from the Steady-State to Potentiodynamic Near-Steady-State. *Anal. Chem.* **2023**, *95*, 9822–9830.
23. Newman, J. Resistance for Flow of Current to a Disk. *J. Electrochem. Soc.* **1966**, *113*, 501–502.
24. Vellzquez, C.S.; Hutchison, J.E.; Murray, R.W. Electrochemical Reactions and Charge Transport in Undiluted Room-Temperature Melts of Oligo(ethylene glycol)-Based Electron Carriers. *J. Am. Chem. Soc.* **1993**, *115*, 7896–7897.
25. Dahms, H. Electronic conduction in aqueous solution. *J. Phys. Chem.* **1968**, *72*, 362–364.

26. Ruff, I.; Friedrich, V.J. Transfer diffusion. I. Theoretical. *J. Phys. Chem.* **1971**, 75, 3297–3302.
27. Lyons, M.E. Transport and kinetics in electroactive polymers. In *Advances in Chemical Physics*; Prigogine, I., Rice, S.A., Eds.; Wiley: New York, NY, USA, 1996.
28. Hyk, W.; Stojek, Z. Generalized Theory of Steady-State Voltammetry without a Supporting Electrolyte. Effect of Product and Substrate Diffusion Coefficient Diversity. *Anal. Chem.* **2002**, 74, 4805–4813.
29. Andrieux, C.P.; Savéant, J.M. Electroneutrality coupling of electron hopping between localized sites with electroinactive counterion displacement. 1. Potential-step plateau currents. *J. Phys. Chem.* **1988**, 92, 6761–6767.
30. Sagara, T.; Tahara, H. Redox of Viologen for Powering and Coloring. *Chem. Rec.* **2021**, 21, 2375–2388.
31. Luong, J.H.T.; Male, K.B.; Zhao, S. Electrochemical Preparation of 1,1'-Dimethylferricinium from a Water-Soluble 1,1'-Dimethylferrocene-2-Hydroxypropyl- $\beta$ -cyclodextrinComplex and Its Applications in Enzyme Assay. *Anal. Biochem.* **1993**, 212, 269–276.
32. Nchimi-Nono, K.; Dalvand, P.; Wadhwa, K.; Nuryyeva, S.; Alneyadi, S.; Prakasam, T.; Fahrenbach, A.C.; Olsen, J.-C.; Asfari, Z.; Platas-Iglesias, C.; et al. Radical-Cation Dimerization Overwhelms Inclusion in [n]Pseudorotaxanes. *Chem. Eur. J.* **2014**, 20, 7334–7344.
33. Wang, X.; Guo, L.; Cao, S.; Zhao, W. Highly stable viologens-based electrochromic devices with low operational voltages utilizing polymeric ionic liquids. *Chem. Phys. Lett.* **2020**, 749, 137434.
34. Correa, C.; Cordoba de Torresi, S.I.; Benedetti, T.M.; Torresi, R.M.; Correa, C.; Cordoba de Torresi, S.I.; Benedetti, T.M.; Torresi, R.M.J. Viologen-functionalized poly (ionic liquids): Spectroelectrochemical and QCM-D studies. *Electroanal. Chem.* **2018**, 819, 365–373.